Supplementary Information for

«REDOX TRANSFORMATIONS AND CATION-CATION INTERACTIONS OF NEPTUNIUM IN ORGANIC SOLUTIONS»

Anna D. Krot, Natalia E. Borisova, Daniil A. Novichkov, Alexander L. Trigub, Alexander M. Fedoseev, Alina A. Sivolap, Mikhail S. Grigoriev, Paulina Kalle, Vladimir G. Petrov, Stepan N. Kalmykov, and Petr I. Matveev

Table of contents

Experimental section

Caution! ^{237}Np is a highly radioactive alpha-emitter ($T_{1/2}$(^{237}Np) = 2·10^{6} years). Its daughter radionuclide ^{233}Pa is a short-lived beta-emitter ($T_{1/2}$(^{233}Pa) = 27 days) with high-energy gamma radiation of 311.9 keV with probability 38.3 % that contributes significantly to its hazardousness. All manipulations with radioactive samples were performed at the specialized facilities in compliance with safety protocols.

1. General procedure of neptunium oxidation state stabilization

Before the extraction experiments, the desired neptunium oxidation state was pre-stabilized according to the following procedures. For Np^{V} preparation, an aliquot of stock solution which contain ~0.25 M of Np^{V} and Np^{VI} (1.7 GBq/L) was taken and diluted 2 times with distilled water. An excess of 0.2 M $NaNO_2$ was added, and the color of the solution immediately turned light green-blue of NpO_2^+. Neptunium (V) hydroxide was precipitated by stepwise addition of concentrated $NH_3{\cdot}H_2O$. The precipitate was washed with distilled water, stirred and centrifuged for at least three times, until the opalescence of the solution became visible. After that, the neptunium (V) hydroxide was dissolved in 1 M HNO_3 or 1 M $HClO_4$ for further use. The concentration of NpO_2^+ was controlled by monitoring the absorbance at 980 nm (ε=400). Np^{VI} was freshly prepared before each experiment by complete evaporating of calculated amount of pre-stabilized NpO_2^+ solution at 237˚C. After evaporation, the residue was maintained at 237˚C in fuming $HClO_4$. The process was completed in ~30 minutes. The residue is then cooled to room temperature and diluted in 1 M HNO_3 to achieve needed concentration. The completeness of oxidation was ensured by the absence of the absorption band of NpO_2^+ at 980 nm. Np^{IV} was obtained by the addition of an excess of NH_2OH and HCl solutions to an aliquot of NpO_2^+ nitric acid solution. The mixture was

maintained at 70°C for approximately 24 hours until the complete reduction of Np^{V} to Np^{IV} was confirmed spectrophotometrically.

2. Synthesis of Ligands

The studied ligands were synthesized according to the previously published method. The ^{1}H and ^{13}C NMR of the prepared compounds matched published data[1,2].

3. Extraction experiments

Organic solution of **Ligand** was added to equal volume of aqueous solution of HNO_3 (or $HClO_4$) with radiometrically detectable concentration of $^{237}NpO_2^+$ (approximately 10^{-4} M) in polypropylene vessel. The vessel was sealed and phases were contacted on a vortex shaker placed in air thermostat at temperature 25±1˚C. After that the phases were separated by centrifugation (10 000 rpm, 2 min). Aliquots of aqueous and organic phases analyzed for ^{237}Np content by gamma spectrometry (Eγ = 29.4 keV) using a high-purity GR 3818 Ge detector with Be window (Canberra Ind.). Distribution ratio (*D*) was calculated by dividing the counting rate in the organic phase by the counting rate in the aqueous phase.

Kinetic experiment. Organic phase contained 0.05 M **Ligand** in F-3 solvent. As an aqueous phase, a solution of 3 M HNO_3 was used. Contact time varied from 2 to 120 min.

Ligand Solvation Numbers. The composition of aqueous phase was 3 M HNO_3 (or $HClO_4$). In organic phase, the concentration of **Ligand** in F-3 varied from 0.001 to 0.05 M. To ensure equilibrium values of distribution ratios, contact time was set to 30 min.

NO_3^- Solvation Numbers. Organic phase contained 0.05 M **Ligand** in F-3. In aqueous phase, the concentration of nitrate ions was controlled by the addition of $LiNO_3$ solution to 0.5 M HNO_3 to achieve total nitrate concentration from 0.5 to 5 M. Contact time was 30 min.

Preparation of references for ^{1}H-NMR and XAS. **Ligand** dissolved in ~350 µl acetonitrile-d_3 was added to 50 µl aqueous solution of $Np(ClO_4)_4$, $NpO_2(ClO_4)$ and $NpO_2(ClO_4)_2$ for references of Np^{IV}, Np^{V} and Np^{VI}, respectively. Concentration of the complex was about $2\cdot10^{-3}$ M.

Sample preparation for ^{1}H-NMR and XAS at $[Np]_{int}=10^{-3}$ M. Organic phase contained 0.05 M **Ligand** in nitrobenzene-d_5. Aqueous phase contained $2\cdot10^{-3}$ M NpO_2^+ (**$Np^{V}_{org.}$** sample) or NpO_2^{2+} (**$Np^{VI}_{org.}$** sample) in 3 M HNO_3. Contact time was 30 min. ^{1}H-NMR and XAS spectra were measured from organic phase within several hours after separation.

Sample preparation for ^{1}H-NMR and XAS at $[Np]_{int}=10^{-2}$ M. Organic phase contained 0.05 M **Ligand** in nitrobenzene-d_5. Aqueous phase contained ~$2\cdot10^{-2}$ M of: NpO_2^+ in 3 M HNO_3 (**$Np^{V}_{org.}$(3 M HNO_3)** sample), NpO_2^+ in 5 M HNO_3 (**$Np^{V}_{org.}$(5 M HNO_3)** sample), NpO_2^{2+} in 3 M HNO_3 (**$Np^{VI}_{org.}$** sample), Np^{4+} in 3 M HNO_3 (**$Np^{IV}_{org.}$** sample). Contact time was 30 min. ^{1}H-NMR and XAS spectra were measured from organic phase within several hours after separation.

4. Crystal data

Preparation of $[LNpO_2NO_3][NpO_2(NO_3)_3]$ (Np66). A solution containing 1 mg (4 µmol) NpO_2^{2+} in methanol was mixed with a solution of 2 mg (4 µmol) **Et-Ligand** in methanol in a glass vial. The resulting solution was isothermally evaporated at 4˚C. After evaporation, red single crystals of **Np66** were isolated for SC-XRD analysis.

Preparation of $[LNpO_2NO_3]_2[NpO_2(NO_3)_4]$ (Np666), $[LNp^{V}O_2NO_3]_2\cdot Np^{VI}O_2(NO_3)_2$ (Np565) and $[^{F}LNp^{V}O_2NO_3]_2\cdot Np^{VI}O_2(NO_3)_2$ (Np565-F). A solution containing 1 mg (4 µmol) NpO_2^{2+} in acetonitrile was mixed with a solution of 2 mg (4 µmol) **oMe-Ligand** in acetonitrile in a glass vial. The resulting solution was isothermally evaporated at 4˚C. After evaporation, precipitate was redissolved in methanol and isothermally evaporated at 4˚C. Dark plate-like single crystals of **Np666** and yellow-green crystals of **Np565** were isolated from one reaction mixture. Similar procedure was repeated with fluorinated **Ligand** and crystals of **Np565-F** were obtained.

Preparation of $[LTh(NO_3)_4]$ (Th4). A solution of 5.7 mg (10 µmol) $Th(NO_3)_4\cdot5H_2O$ in $CHCl_3$ was mixed with a solution of ~5 mg (10 µmol) **Et-Ligand** in acetonitrile in a glass vial. The resulting solution was isothermally evaporated at room temperature.

The data for all neptunium crystals were collected on a Bruker Kappa APEX II diffractometer with a CCD area detector and for **Th4** on a Bruker Smart Photon II diffractometer using graphite-monochromatized Mo$K\alpha$ (λ = 0.71073 Å) radiation at 100 K. Cell refinement and data reduction were conducted using the software SAINT (Bruker). The data were corrected for Lorentz and polarization effects, and absorption correction based on measurements of equivalent reflections was applied using SADABS[3]. The structures were solved by direct methods (SHELXT 2018/2) and refined by full matrix least-squares on F^2 (SHELXL 2018/3) with anisotropic

displacement parameters for all non-hydrogen atoms[4,5]. Hydrogen atoms were placed in calculated positions and refined using a riding model. In **Np565-F** one fluorine atom is disordered over two *ortho*-positions with the refined ratio 0.8/0.2; in **Np565** one of the *o*-tolyl rings is disordered over two positions with equal occupancies; in **Th4** one *p*-ethyl group is disordered over two positions with equal occupancies. In the structure of **Np565-F** highly disordered solvent molecules (acetonitrile) could not be modeled and the PLATON SQUEEZE procedure was used to account the contribution of these solvent molecules to the structure factors[6]. Crystallographic details are presented in Tables 3-5. For molecular graphics Olex2 1.5 was used[7].

Table S1. Crystallographic details for **Np66** and **Np666** structures.

Identification code	**Np66**	**Np666**[a)]
CCDC number	2395322	2395325
Empirical formula	$C_{32}H_{34}N_8Np_2O_{18}$	$C_{60}H_{60}N_{14}Np_3O_{28}$
Formula weight	1292.67	2136.22
Crystal system	monoclinic	triclinic
Space group	$P2_1/n$	P-1
a/Å	15.9713(7)	8.1227(13)
b/Å	11.3635(5)	17.534(3)
c/Å	22.5333(9)	25.389(4)
α/°	90	106.001(7)
β/°	98.939(1)	92.587(7)
γ/°	90	94.446(7)
Volume/Å^3	4039.9(3)	3457.1(10)
Z	4	2
ρ_{calc}g/cm^3	2.125	2.052
μ/mm^{-1}	5.201	4.571
F(000)	2448.0	2042.0
Crystal size/mm^3	0.32 × 0.18 × 0.14	0.32 × 0.05 × 0.02
2Θ range for data collection/°	6.86 to 59.998	8.294 to 49.998
Reflections collected	75724	36429
Independent reflections	11748 [R_{int} = 0.0344, R_{sigma} = 0.0247]	12103 [R_{int} = 0.2227, R_{sigma} = 0.2785]
Data/restraints/parameters	11748/0/545	12103/255/870
Goodness-of-fit on F^2	1.045	1.001
Final R indexes [I>=2σ (I)]	R_1 = 0.0194, wR_2 = 0.0365	R_1 = 0.0954, wR_2 = 0.1686
Final R indexes [all data]	R_1 = 0.0259, wR_2 = 0.0382	R_1 = 0.2265, wR_2 = 0.2159
Largest diff. peak/hole / e Å^{-3}	0.71/-0.86	2.45/-2.35

[a)] The precision of geometric parameters is low and the data is used only to establish connectivity and identity.

Table S2. Crystallographic details for **Np565** and **Np565-F** structures.

Identification code	**Np565**	**Np565-F**
CCDC number	2395324	2395323
Empirical formula	$C_{64}H_{66}N_{14}O_{22}Np_3$	$C_{60}H_{54}F_4N_{14}Np_3O_{22}$
Formula weight	2094.30	2110.17
Crystal system	monoclinic	triclinic
Space group	C2/c	P-1
a/Å	28.1405(18)	11.1713(3)
b/Å	13.4506(8)	11.5817(4)
c/Å	22.622(2)	13.7244(4)
α/°	90	85.634(2)
β/°	123.760(2)	89.208(2)
γ/°	90	63.655(2)
Volume/Å^3	7118.7(9)	1586.26(9)
Z	4	1
ρ_{calc}g/cm^3	1.954	2.209
μ/mm^{-1}	4.432	4.981
F(000)	4012.0	1003.0

Crystal size/mm^3	0.16 × 0.14 × 0.1	0.2 × 0.2 × 0.15
2Θ range for data collection/°	8.19 to 54.994	6.88 to 54.998
Reflections collected	52580	20669
Independent reflections	8140 [R_{int} = 0.1123, R_{sigma} = 0.0788]	7226 [R_{int} = 0.0371, R_{sigma} = 0.0426]
Data/restraints/parameters	8140/74/451	7226/1/448
Goodness-of-fit on F^2	1.044	1.027
Final R indexes [I>=2σ (I)]	R_1 = 0.0512, wR_2 = 0.0873	R_1 = 0.0262, wR_2 = 0.0551
Final R indexes [all data]	R_1 = 0.0768, wR_2 = 0.0962	R_1 = 0.0339, wR_2 = 0.0582
Largest diff. peak/hole / e Å^{-3}	1.59/-1.33	1.45/-0.94

Table S3. Crystallographic details for **Th4** structure.

Identification code	**Th4**
CCDC number	2395348
Empirical formula	$C_{32}H_{34}N_8O_{14}Th$
Formula weight	986.71
Crystal system	monoclinic
Space group	C2/c
a/Å	51.304(4)
b/Å	8.5529(7)
c/Å	17.5571(14)
α/°	90
β/°	101.537(3)
γ/°	90
Volume/Å^3	7548.3(10)
Z	8
ρ_{calc}g/cm^3	1.737
μ/mm^{-1}	4.028
F(000)	3872.0
Crystal size/mm^3	0.4 × 0.4 × 0.08
2Θ range for data collection/°	4.688 to 53.99
Reflections collected	56261
Independent reflections	8225 [R_{int} = 0.0761, R_{sigma} = 0.0486]
Data/restraints/parameters	8225/7/501
Goodness-of-fit on F^2	1.039
Final R indexes [I>=2σ (I)]	R_1 = 0.0330, wR_2 = 0.0685
Final R indexes [all data]	R_1 = 0.0490, wR_2 = 0.0763
Largest diff. peak/hole / e Å^{-3}	1.75/-1.58

5. Infrared spectroscopy measurements

Infrared spectra of the samples were recorded using the FT-801 IR Fourier spectrometer (Simex, Russia). Crystals were mixed with NaCl in mass ratio ~1:100. NaCl was used instead of KBr to avoid redox transformations when pressing the pellets. For each spectrum, 16 scans were recorded in the range from 500 to 4500 cm^{-1} with spectral resolution of 4 cm^{-1}.

6. XAS measurements

X-ray absorption measurements of organic solutions with $[Np]_{int}=10^{-2}$ M were performed at STM beamline of Kurchatov Synchrotron Radiation Source (Moscow, Russia)[8]. Samples of neptunium complexes in aqueous and organic solutions in nitrobenzene-d_5 and acetonitrile-d_3 were placed in polypropylene tubes and doubly confined. Holders with the samples were placed between 1st and 2nd ionization chambers, and Np^V reference (powder of $NaNpO_2CO_3$) was placed between 2nd and 3rd for energy calibration. XAS spectra at Np L_3 edge were measured at room temperature in the fluorescence mode, monochromatization of the beam achieved using Si (220). For each sample, 7-10 scans were measured to ensure high enough signal-to-noise ratio and avoid beam damage. For XAS data processing, IFFEFIT software package was used[9]. The maximum of the first

derivative of Np^V reference was calibrated to 17613.4 eV[10] in ATHENA program. For each sample, 7-10 scans were averaged and calibrated using the energy position of reference. EXAFS fitting was performed in ARTEMIS program in k range 3-13 $Å^{-1}$, R range 1-4 Å. The fitting was carried out in R space, with k weights 2 and 3. Phase shifts and amplitudes were calculated using **Np66** crystal structure with FEFF8.5L code[11]. The shift of the threshold energy, ΔE_0 parameter, was the same for all coordination shells and varied as a global parameter. Amplitude reduction factor S_0^2 was set to 0.9. Coordination numbers were fixed according to the proposed crystal structure. Multiple scattering paths $O_{ax.}$-Np-$O_{ax.}$ was taken into account every time with $\Delta R=2\Delta R(Np\text{-}O_{ax.})$ and $\sigma^2 = 2\sigma^2$ ($Np\text{-}O_{ax.}$).

For XAS measurements of organic solutions with $[Np]_{int}=10^{-2}$ M, specialized holders were fabricated using a photopolymer 3D printer (Anycubic Photon M3 Max). The external dimensions of the rectangular holder are 30 × 40 mm, and thickness 3 mm, optimized for achieving a significant absorption edge step. Internal dimensions of the holder were 15 × 15 mm to ensure that the X-ray beam fully covered the sample area. The windows of the holder were covered with two layers of Kapton. Organic solutions were injected into the holder, confined and placed into additional holder, which was installed in the laboratory spectrometer at the detector slits. Placing the samples at the detector slits was essential to ensure the passage of only the monochromatic beam through the sample, thereby preventing the influence of the full X-ray tube spectrum and avoiding radiation damage.

X-ray absorption measurements of organic solutions with $[Np]_{int}=10^{-2}$ M were conducted using the laboratory X-ray spectrometer at the Department of Radiochemistry, Lomonosov Moscow State University[12]. The spectrometer employs a Rowland circle geometry with a Johann-type crystal monochromator. An Ag anode X-ray tube operating at 1.5 kW was used as the X-ray source, set to 35 kV and 20 mA. Photon detection was carried out using an Amptek X-123 (FASTSDD) silicon drift detector. XAS measurements at Np L_3 edge were performed using a Ge (999) SBCA crystal monochromator with a 0.5 m bending radius. The scanning range was from 17550 to 17700 eV with a step size of 1 eV and a collection time of 6 seconds per energy point. To obtain high-quality experimental data, 12 scans were recorded for each sample. The I_0 signal was obtained by measurements of empty holder identical to the one used for the sample.

7. ^{1}H-NMR measurements

The NMR spectra were measured with a BRUKER AVANCE-600 MHz NMR spectrometer at 298±0.3K in 5 mm probe tubes (with the solvents as internal reference). The 2D homonuclear shift correlation using gradient pulse for selection experiments were made for protons assignment.

8. Computational details

Optimization and frequency calculations were performed at the PBE-D3BJ[13,14] /ECP60MWB[15–17] on Np and ma-def2-SVP on other elements, using the CPCM solvation model with acetonitrile and water as solvents. To improve energy, we performed single-point (SP) energy calculations with the relativistic X2C Hamiltonian, the PBE0-D3BJ functional, the X2C-TZVPall basis set[18,19] for all elements, and the cc-pVTZ-X2C basis set for the Np atom. All structures are characterized by the absence of imaginary frequencies, except for CCI structure $[LNp^VO_2NO_3]_2{\cdot}Np^{VI}O_2(NO_3)_2$. Due to the extraordinarily complex wavefunction behavior and large size, it could not be resolved with analytical approaches to determine its frequencies. Therefore, for this structure only optimization was performed, and its electronic energy was used for further calculations.

To investigate the complex electronic structure of the Np complexes, we performed basic bonding analysis. We calculated Hirshfeld and Merz-Kollman charges, as previously utilized in refs[20,21] and conducted QTAIM bonding analysis, which has been effectively applied to structures with complex bonding behavior, as demonstrated in refs[22,23].

9. XANES calculations

The modeling of the Np L_3 edge XANES was carried out using the FDMNES code[24]. The simulation parameters were optimized to achieve the best agreement with standard-resolution XANES. Spin-orbit coupling and relativistic effects were included. The Fermi energy was estimated using a self-consistent field (SCF) cycle, which only involved the first coordination shell of oxygen around the absorbing neptunium atom. The projected density of states (DOS) on the absorber was also calculated. A correction of 0.5 eV was applied to all simulations to adjust the Fermi energy, ensuring that it did not overlap with the Np f-states and O p-states. The core level width and convolution broadening were set to 5 eV each to obtain simulations comparable with our experimental data. The cluster radius was 5 Å, and results were obtained using the Green's function method.

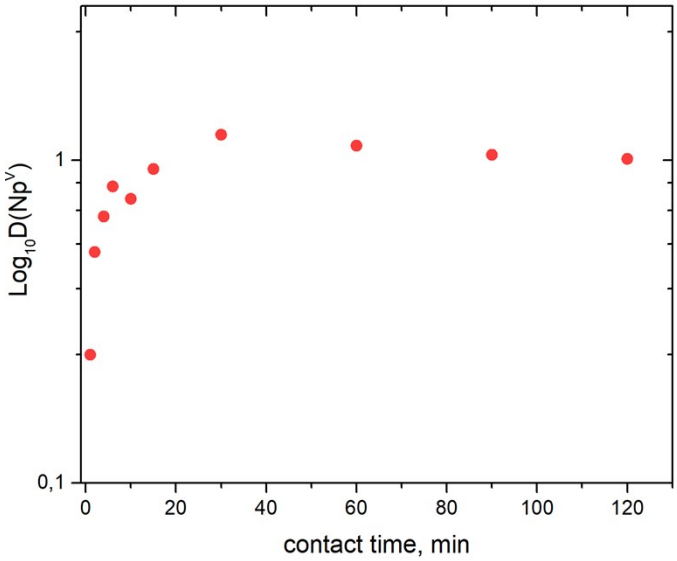

Figure S1. Extraction kinetics of NpO_2^+, [L]=0.05 M in F-3, aqueous phase: 3 M HNO_3, T=298 K.

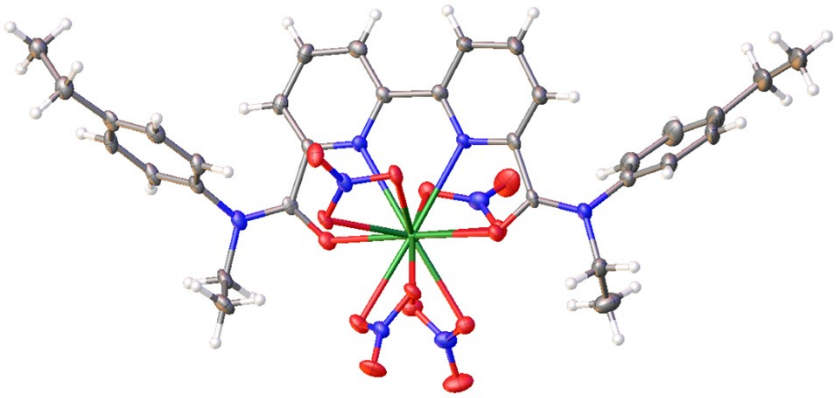

Figure S2. Crystal structure of $LTh(NO_3)_4$ (**Th4**). Thermal ellipsoids are shown at the 50% probability level. Color code: green – thorium, red – oxygen, blue – nitrogen, grey – carbon, white – hydrogen, light green – fluorine.

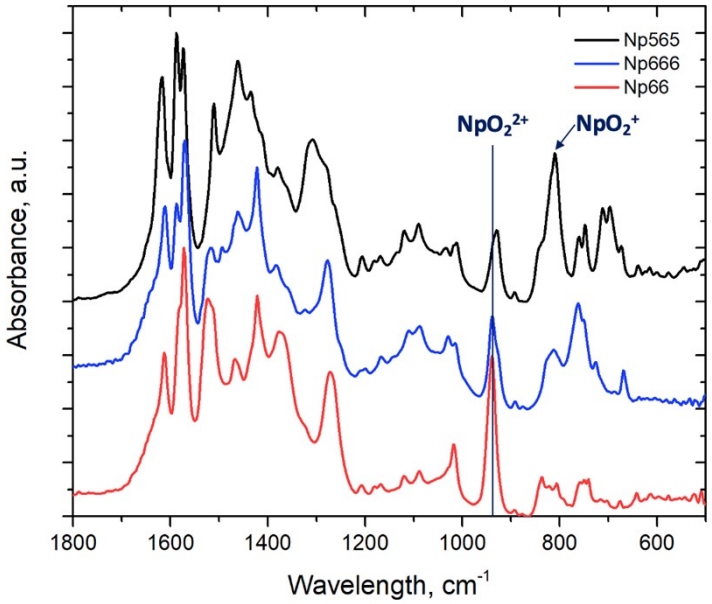

Figure S3. IR spectra of **Np66**, **Np666** and **Np565**.

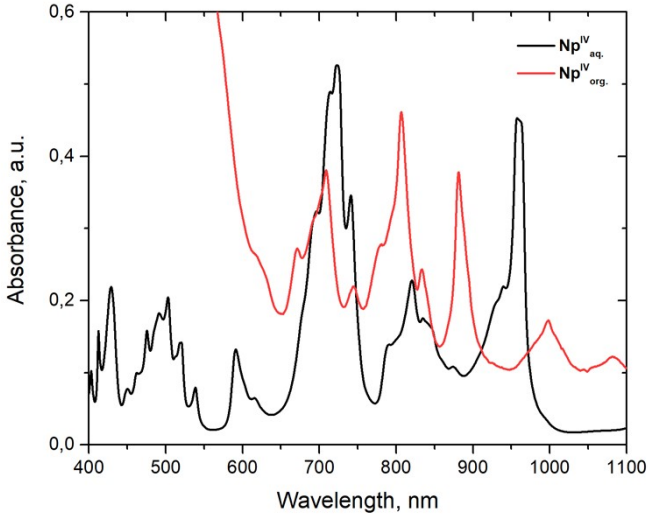

Figure S4. Np^{IV} UV-vis absorption spectra of initial Np^{4+} in 3 M HNO_3 solution ($Np^{IV}_{aq.}$) and of organic solution after extraction with 0.05 M **Ligand** in $PhNO_2$ ($Np^{IV}_{org.}$). For clarity, $Np^{IV}_{aq.}$ Spectrum is divided by 3 and $Np^{IV}_{org.}$ spectrum is multiplied by 2.5.

^{1}H-NMR data

Table S4. NMR assignments

Complex	Solvent	3-Py	4-Py	5-Py	2,6-Ar	3,5-Ar	EtAr	EtN
$LNp^{IV}(ClO_4)_4$	CH_3CN-d_3	12.92	9.85	5.87	11.83	8.94	3.58 (CH_2) 1.91 (CH_3)	16.36 (CH_2) 6.05 (CH_3)
$LNp^{V}(ClO_4)$	CH_3CN-d_3	-9.32*; -19.53*; -25.08*			–	4.73*	0.29 (CH_2) -0.71 (CH_3)	-31.52* (CH_2) -8.86* (CH_3)
$LNp^{VI}(ClO_4)_2$	CH_3CN-d_3	1.15	3.82	-1.17	5.27	6.29d	1.89q (CH_2) -0.54t (CH_3)	-5.31 (CH_2) -1.60 (CH_3)
$Np^{V}_{org.}$ 10^{-3} M	$PhNO_2$ LNp^{VI}: 0.06 mol%	1.15d	3.86t	-0.85d	5.72d	6.47d	2.61q (CH_2) 0.57t (CH_3)	-5.37 (CH_2) -1.33 (CH_3)
$Np^{VI}_{org.}$ 10^{-3} M	$PhNO_2$ LNp^{VI}: 0.09 mol%	1.11 d	3.87t	-0.84d	5.72d	6.47d	2.61q (CH_2) 0.57t (CH_3)	-5.37 (CH_2) -1.34 (CH_3)
$Np^{V}_{org.}$ 10^{-2} M (3 M HNO_3)	$PhNO_2$ LNp^{VI}: 100 mol%	1.14d	3.92	-0.73	5.75	6.47	* 0.55t (CH_3)	-5.22 (CH_2) -1.33 (CH_3)
	LNp^{V}: trace	-8.05, -18.05, -21.14						-28.90 (CH_2) -8.05 (CH_3)
$Np^{V}_{org.}$ 10^{-2} M (5 M HNO_3)	$PhNO_2$ LNp^{VI}: 100 mol%	1.13d	3.87t	-0.76d	5.73d	6.45d	* 0.55t (CH_3)	-5.24 (CH_2) -1.33 (CH_3)
$Np^{VI}_{org.}$ 10^{-2} M	$PhNO_2$	1.25d	3.92t	-0.72d	5.75d	6.46d	2.48q	-5.21

	LNp^{VI}: 100 mol%						(CH_2) 0.57t (CH_3)	(CH_2) -1.33 (CH_3)
Dissolved **Np565**	CH_3CN-d_3	-7.70, -18.59, -22.28						-29.56 (CH_2) -8.45 (CH_3)

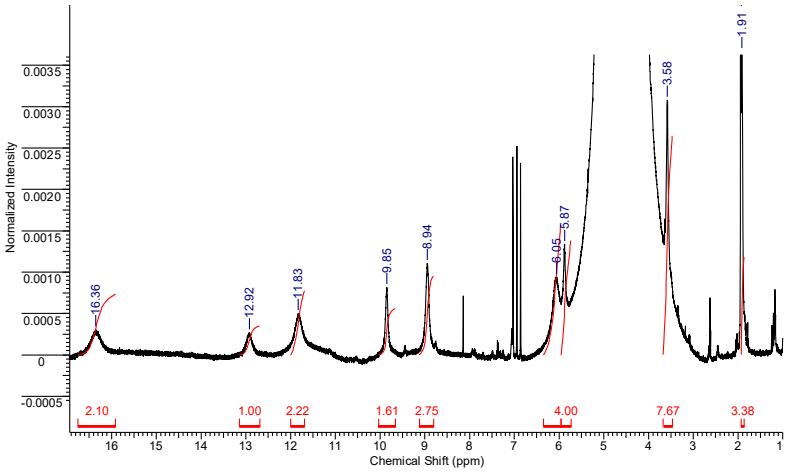

Figure S5. ^{1}H-NMR spectrum of $LNp^{IV}(ClO_4)_4$ complex in acetonitrile-d_3.

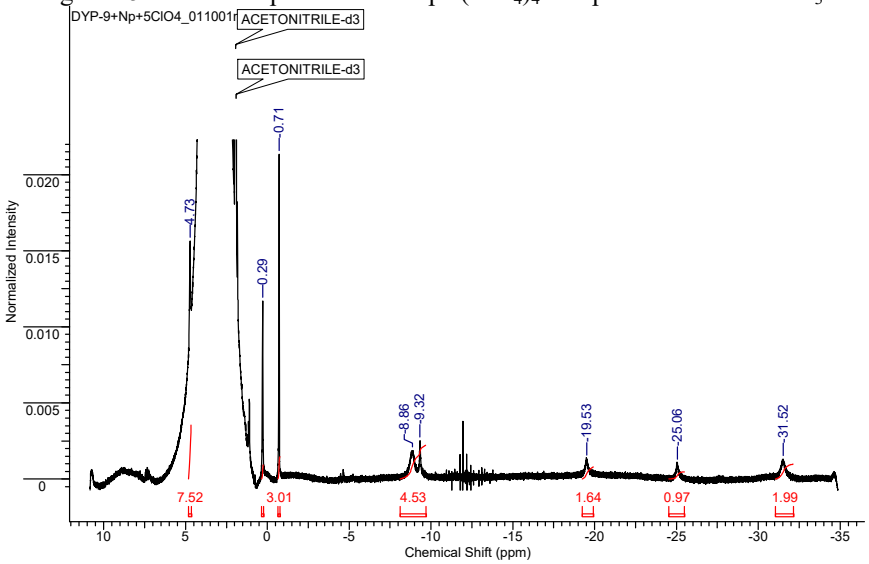

Figure S6. ^{1}H-NMR spectrum of $LNp^{V}(ClO_4)$ complex in acetonitrile-d_3.

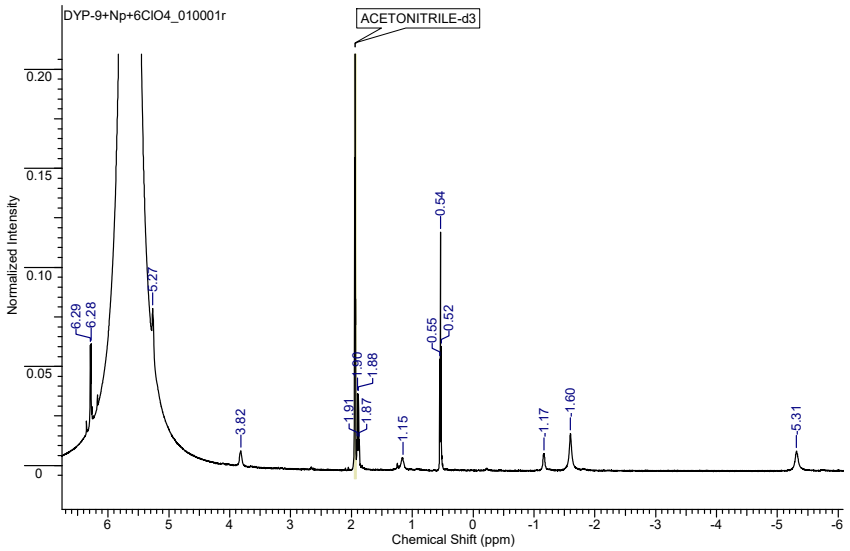

Figure S7. ^{1}H-NMR spectrum of $LNp^{VI}(ClO_4)_2$ complex in acetonitrile-d_3.

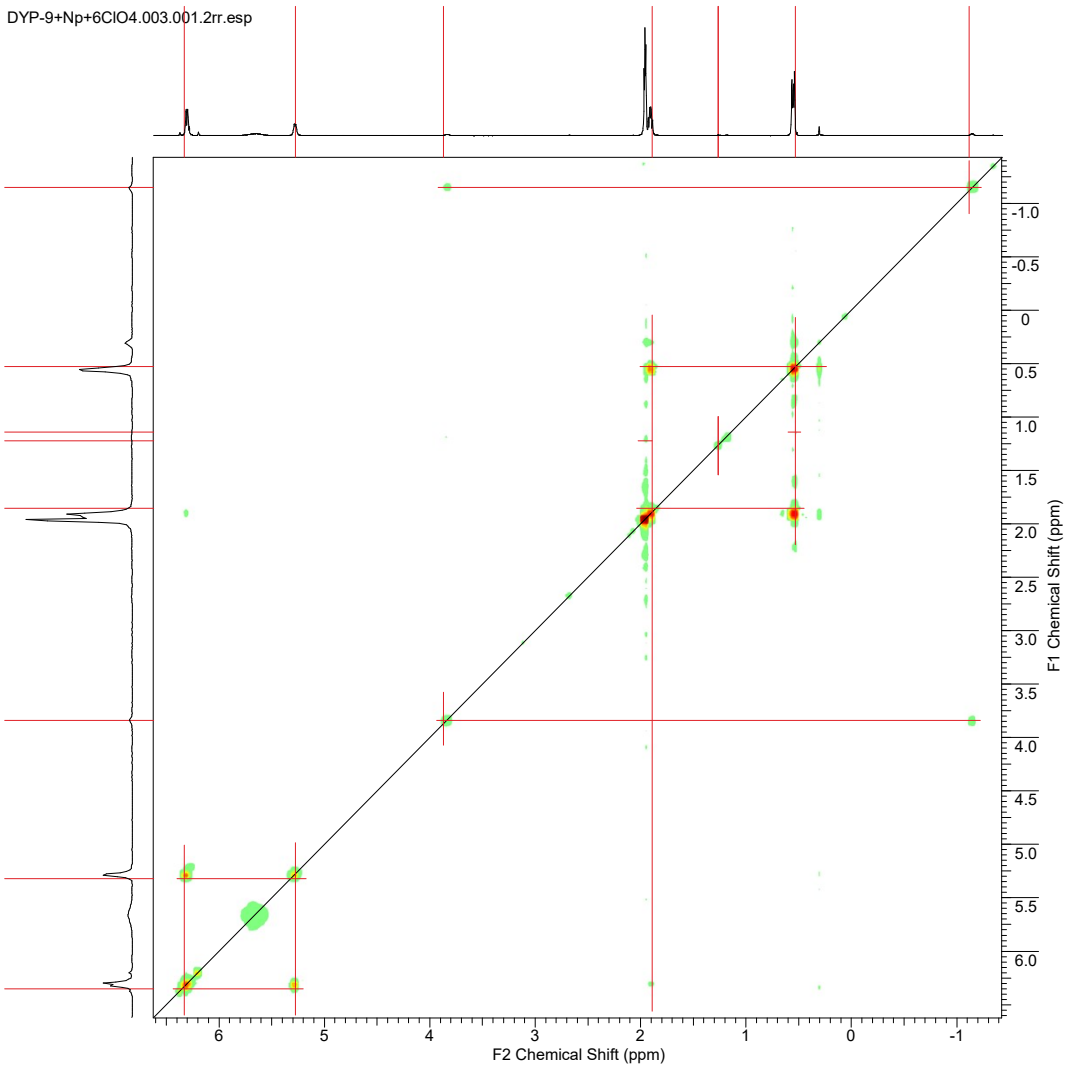

Figure S8. 2D COSY spectrum of $LNp^{VI}(ClO_4)_2$ complex in acetonitrile-d_3.

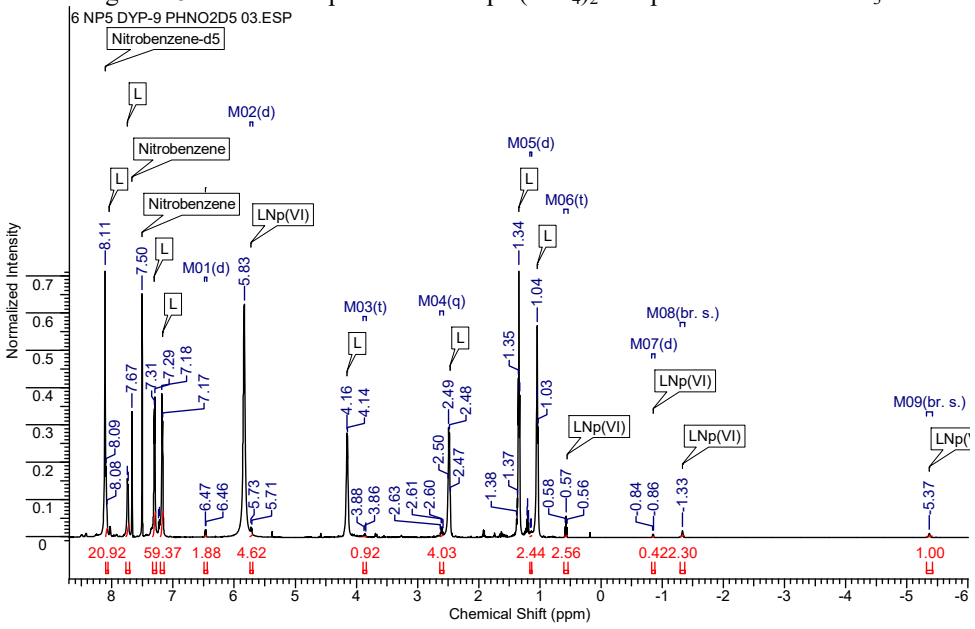

Figure S9. ^{1}H-NMR spectrum of $\mathbf{Np^{V}_{org.}}$ sample ([$Np_{int.}$]=10^{-3} M). Region with negative chemical shifts is magnified in the Main Text (Figure 7).

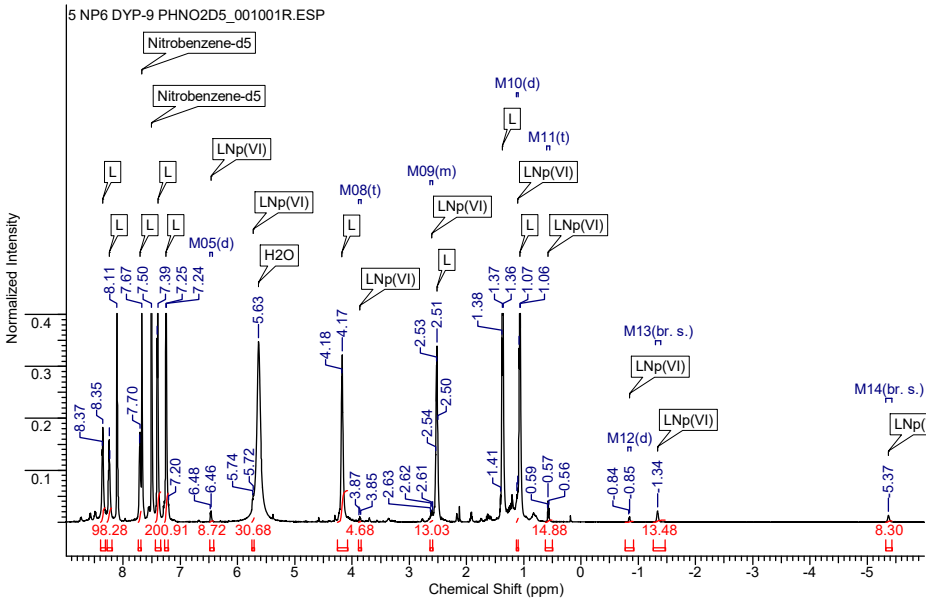

Figure S10. ^{1}H-NMR spectrum of $\mathbf{Np^{VI}_{org.}}$ sample ([$Np_{int.}$]=10^{-3} M).

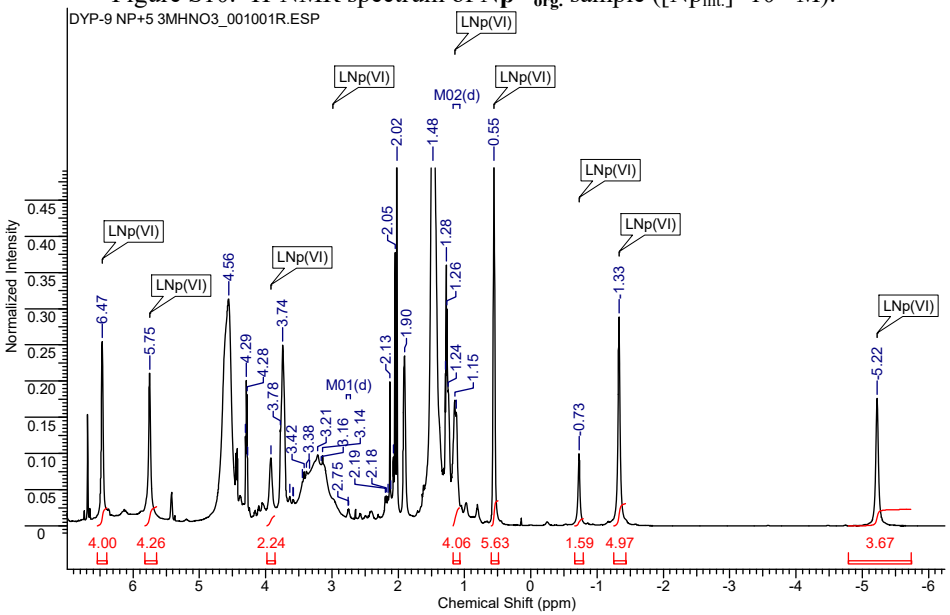

Figure S11. ^{1}H-NMR spectrum of $\mathbf{Np^{V}_{org.}(3\ M\ HNO_3)}$ sample ([$Np_{int.}$]=10^{-2} M).

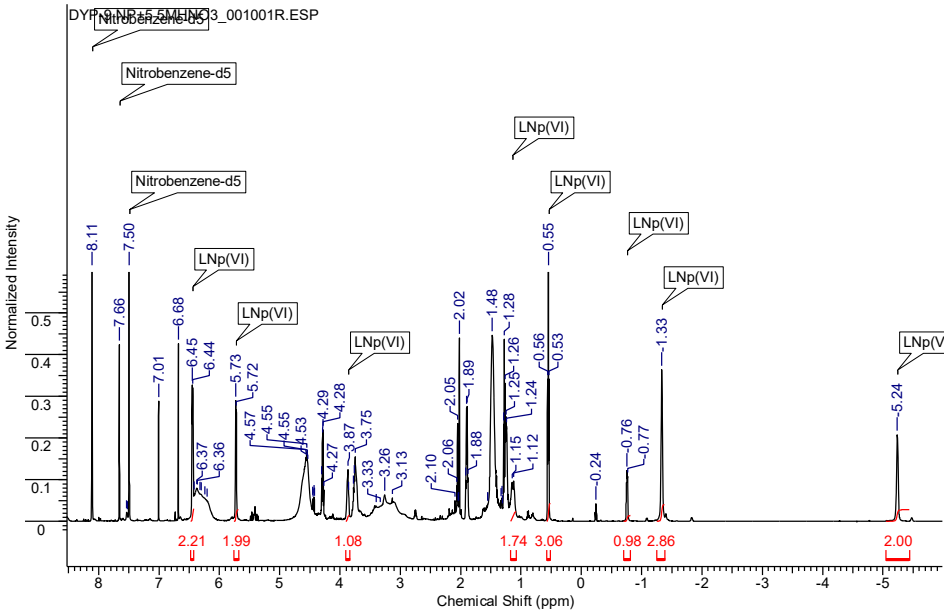

Figure S12. ^{1}H-NMR spectrum of **$Np^{V}_{org.}$(5 M HNO_3)** sample ([$Np_{int.}$]=10^{-2} M).

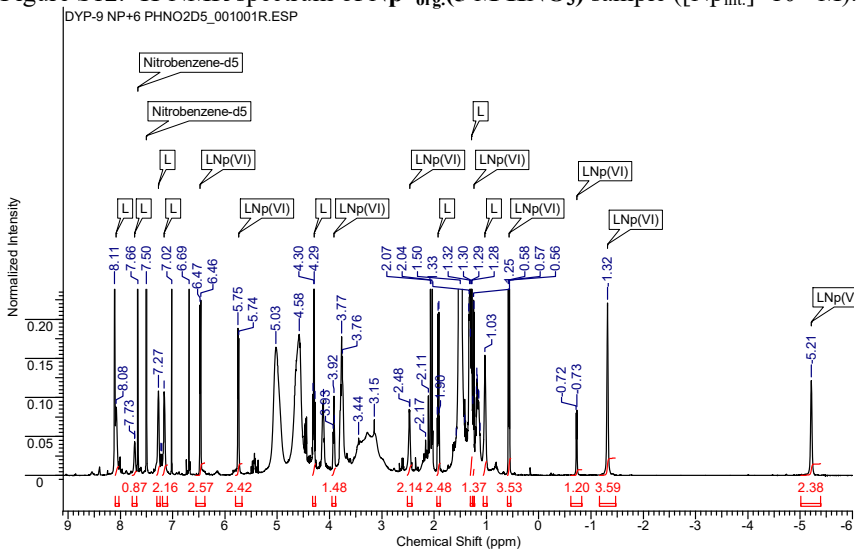

Figure S13. ^{1}H-NMR spectrum of **$Np^{VI}_{org.}$** sample ([$Np_{int.}$]=10^{-2} M).

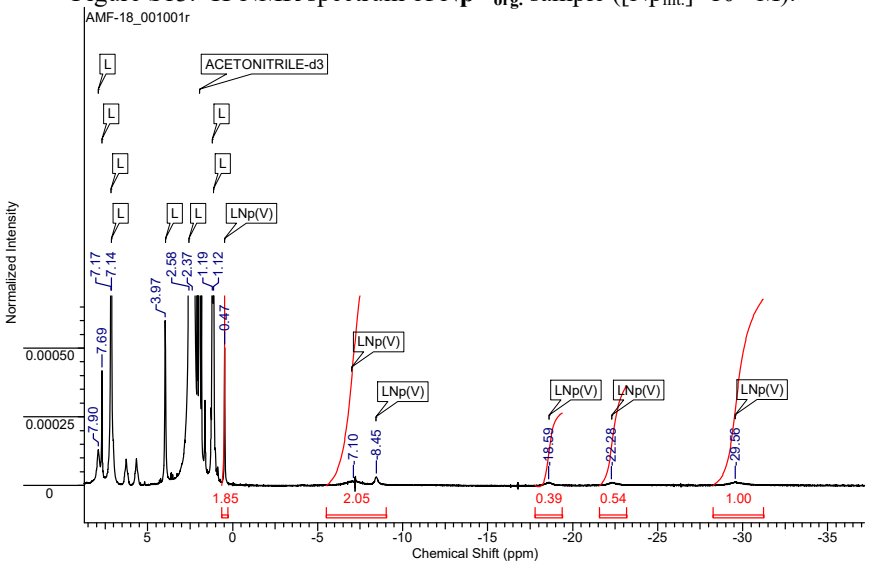

Figure S14. ^{1}H-NMR spectrum dissolved **Np565** in acetonitrile-d_3.

EXAFS fitting parameters

Table S2. Best fit parameters of the EXAFS spectra of $Np^{V}_{org.}$ and $Np^{VI}_{org.}$ samples.

	$Np^{V}_{org.}$ sample: $[LNp^{VI}O_2NO_3]NO_3$			**$Np^{VI}_{org.}$ sample: $[LNp^{VI}O_2NO_3]^{+}$+$[Np^{VI}O_2(NO_3)_3]^{-}$**		
	CN	**R, Å**	**σ^2, Å^2**	**CN**	**R, Å**	**σ^2, Å^2**
ΔE_0, eV		8.4			7.9	
R-factor		0.007			0.016	
Np-O_{ax}	**2**	1.77	0.0015	**2=(2+2)/2**	1.77	0.0026
Np-O_{lig}	**2**	2.37	0.005	**1=(2+0)/2**	2.36	0.003
Np-O_{NO3}	**2**	2.49	0.008	**4=(2+6)/2**	2.50	0.008
Np-N_{phen}	**2**	2.59	0.005	**1=(2+0)/2**	2.58	0.003
Np-N_{phen}	**1**	2.96	0.003	**2=(1+3)/2**	3.0	0.006
Np-C_{phen}-1	**2**	3.27	0.007	**1=(2+0)/2**	3.36	0.003
Np-C_{phen}-2	**4**	3.48		**2=(4+0)/2**	3.44	
MS[a])(O_{ax}-Np-O_{ax})	**2**	3.54	0.003	**2**	3.54	0.005
Np-O_{NO3}	**1**	4.18	0.003	**2=(1+3)/2**	4.14	0.003
MS(O-N, N-O-N)	**2, 1**	4.18	0.003	**4, 2**	4.14	0.003

[a]) MS – multiple scattering.

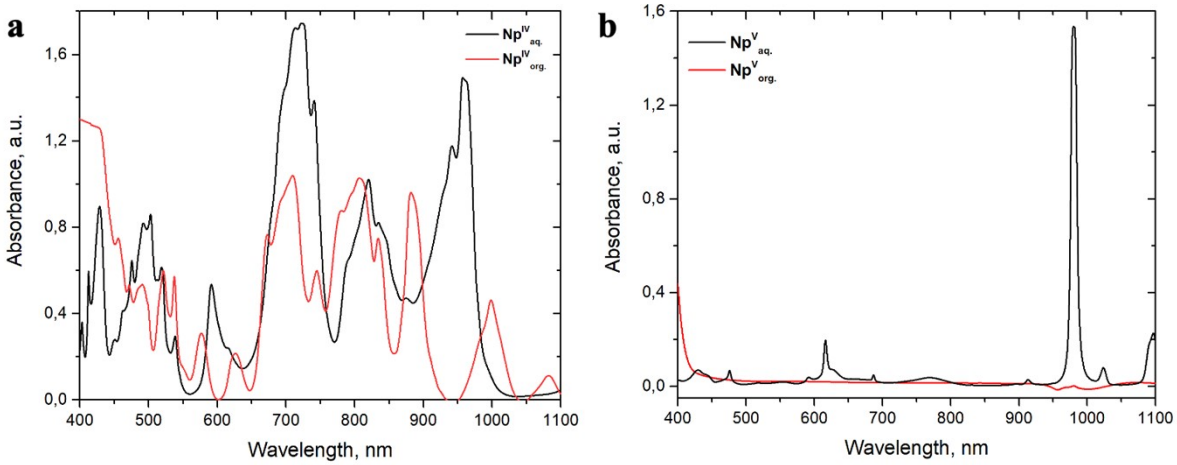

Figure S15. UV-vis spectra of the initial aqueous and organic phases after the extraction. Aqueous phase: [Np]=0.01 M in 3 M HNO_3; organic phase: 0.05 M **Ligand** in $PhNO_2$-d_5. Initial oxidation state of Np in aqueous solution is Np^{IV} (a) and Np^{V} (b).

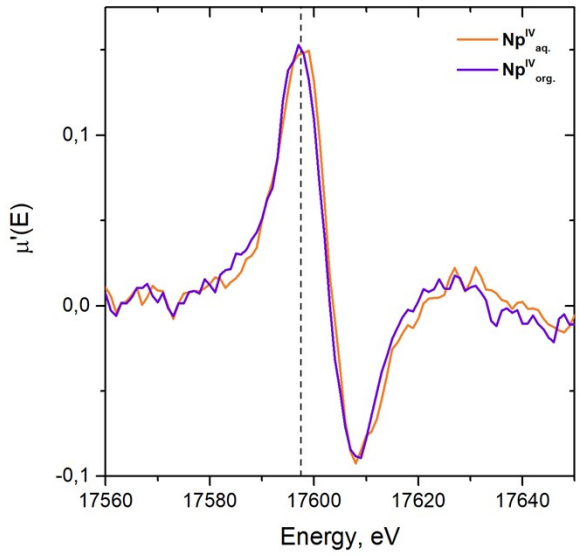

Figure S16. First derivatives of XANES spectra of the initial aqueous phase ($Np^{IV}_{aq.}$) and organic phase after extraction ($Np^{IV}_{org.}$), initial [Np^{IV}] is ~0.01 M.

XANES calculations

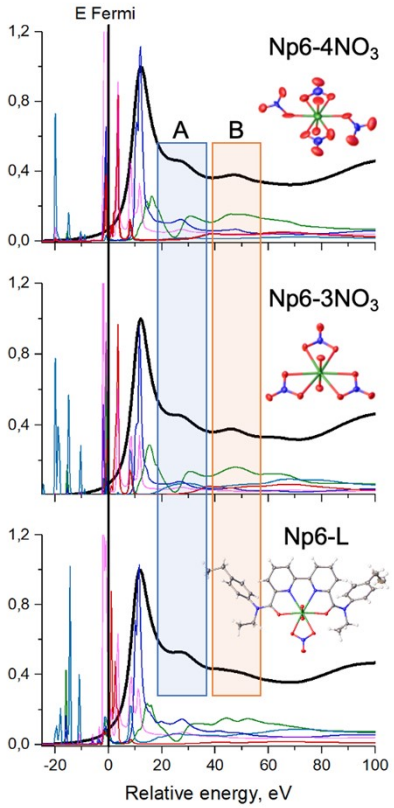

Figure S17. Calculated XANES spectra of the displayed structural models and projected density of states. Color code: black – theoretical XANES spectrum, green – sDOS Np, light blue – pDOS Np, blue – dDOS Np, red – fDOS Np, pink – pDOS O_{ax}.

Figure S17 shows calculated density of states (DOS) for neptunium and oxygen in three different complexes taken from crystal structures: $[NpO_2(NO_3)_4]^{2-}$ ("Np6-4NO_3"), ($[NpO_2(NO_3)_3]^-$ ("Np6-3NO_3"), and $[LNpO_2(NO_3)]^+$ ("Np6-L"). Neptunium d-DOS play a significant role in the unoccupied states (above the Fermi level). Particularly, main contribution in the absorption edge region and near the post-edge feature A comes from the neptunium d-states. The intensity of these states increases in the order Np6-3NO_3<Np6-4NO_3<Np6-L, which leads to an increase in the intensity of feature A in the same order. The main contribution to the energy region around 50 eV above the Fermi level (feature B), comes from neptunium s-states. As the structural model changes

from nitrate anionic complexes Np6-3NO_3 and Np6-4HNO_3 to Np6-L, a noticeable reduction in their contribution to the overall DOS is observed and therefore significant decrease in the intensity of the spectral feature B.

The relationship between the structure of a complex and the intensity of features A and B in the XANES spectrum can be used to infer which structural changes occur based on the shape of the spectrum. XANES spectra measured from $\mathbf{Np^{V}_{org.}}$ and $\mathbf{Np^{VI}_{org.}}$ samples at $[Np^{VI}]_{int}=10^{-2}$ M and 10^{-3} M are compared in Figure 18. The shape of the spectra of extracted complexes with initial Np^{V} oxidation state is similar, suggesting that the neptunium speciation is also similar. Noticeable differences are observed between $\mathbf{Np^{VI}_{org.}}$ samples at $[Np^{VI}]_{int}=10^{-2}$ M and 10^{-3} M. The intensity of feature B is decreased when neptunium concentration is increased. Modelling of XANES spectra (Figure S17) demonstrate that feature B is more pronounced in nitrate-coordinated anionic complexes of NpO_2^{2+}. According to EXAFS data, neptunium complex formed at $[Np]_{int}=10^{-3}$ M is $[LNp^{VI}O_2NO_3][Np^{VI}O_2(NO_3)_3]$, which contains 1/2 of total neptunium atoms in trinitrate coordination. From this we can assume that when the initial neptunium concentration is increased, complex with smaller content of anionic nitrate-coordinated part is formed. An example of such complex is **Np666**, in which 1/3 of total neptunium atoms is nitrate coordinated. Additional confirmation of the formation of anionic species when Np^{VI} is extracted is provided by the decreased intensity of feature A in comparison to $\mathbf{Np^{V}_{org.}}$ samples. According to XANES modeling results, decrease of feature A intensity signifies the decrease of Np6-L fraction. Although the shape of XANES allow to deduce the qualitative changes in complex composition, EXAFS measurements are needed for strict quantitative determination of neptunium speciation.

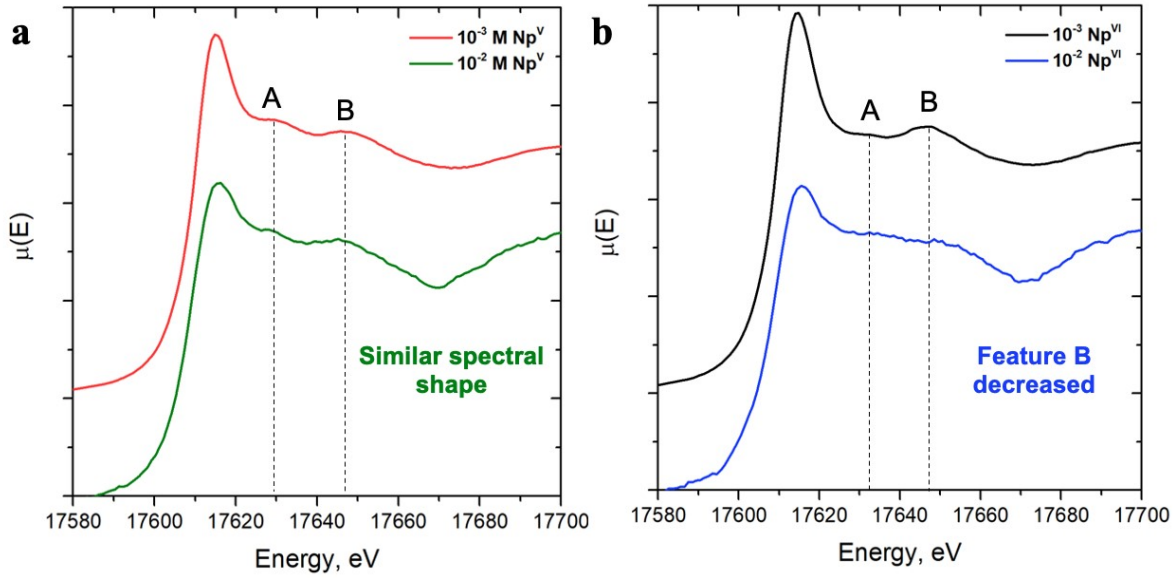

Figure S18. XANES spectra of organic solutions after the extraction from $[Np]_{int}=10^{-3}$ M and $[Np]_{int}=10^{-2}$ M, with initial oxidation states Np^{V} (a) and Np^{VI} (b).

Comparison between XRD and DFT geometries

Table S3. Bond lengths in SC structures and optimized geometries.

Bond	Crystal structure	DFT
$LNp^{V}O_2NO_3$[a]		
Np-O_{NpO2}	–	1.817-1.819
Np-O_{CO}	–	2.499-2.512
Np-$O_{nitrate}$	–	2.622-2.633
Np-N_{phen}	–	2.594-2.623
$[LNp^{VI}O_2NO_3]NO_3$[a]		
Np-O_{NpO2}	1.753-1.753	1.774-1.776
Np-O_{CO}	2.362-2.395	2.370-2.373
Np-$O_{nitrate}$	2.505-2.522	2.566-2.567
Np-N_{phen}	2.586-2.591	2.615-2.620
$[LNp^{VI}O_2NO_3][Np^{VI}O_2(NO_3)_3]$		
Np-O_{NpO2}	1.753-1.753	1.770-1.775
Np-O_{CO}	2.362-2.395	2.353-2.364

Np-$O_{nitrate}$	2.505-2.522	2.556-2.563
Np-N_{phen}	2.586-2.591	2.613-2.618
Np-$O_{nitrate,Np(NO3)3}$	2.445-2.465	2.468-2.475
$[LNp^{V}O_2NO_3]_2Np^{VI}O_2(NO_3)_2$		
Np-O_{NpO2}	1.795-1.866	1.797-1.826
Np-$O_{briging,central\ Np}$	2.344-2.344	2.509-2.512
Np-O_{CO}	2.452-2.452	2.427-2.437
Np-$O_{nitrate}$	2.584-2.601	2.584-2.587
Np-N_{phen}	2.655-2.658	2.626-2.629

[a] The corresponding SC structure was not obtained and a fragment of **Np66** structure was taken for DFT calculations.

Charges

Additionally, we decided to reveal how the how oxidation state of Np affects its interaction with nitrates and the Ligand in the first coordination sphere. We performed two well-established approaches – the calculation of Hershfield charges (C16 model) and the evaluation of bond properties according to the QTAIM model.

Table S4. CH5/MK charges, QTAIM analysis with electron density/Laplacian of electron density (a. u.).

	$LNp^{V}O_2NO_3$	$[LNp^{VI}O_2NO_3]NO_3$	$[LNp^{VI}O_2NO_3][Np^{VI}O_2(NO_3)_3]$
Charge on Np	1.630/ 1.535	2.064/1.532	2.076/1.519 – cation 2.077/1.812 – anion
Charge on O_{NpO2}	-0.855/-0.722	-0.752/-0.458	-0.753/-0.458 – cation -0.741/-0.509 – anion
Charge on N_{phen}	-0.341/-0.467	-0.337/-0.420	-0.339/-0.409
Charge on O_{CO}	-0.340/-0.412	-0.363/-0.392	-0.357/-0.391
Charge on nitrate	-0.645/-0.768	-0.552/-0.640	-0.556/-0.650 - cation
Np-N_{phen}	0.044/0.146	0.046/0.141	0.046/0.133
Np-O_{CO}	0.047/0.180	0.067/0.286	0.069/0.249
Np-$N_{nitrate}$	0.037/0.143	0.048/0.169	0.046/0.156 - cation

XYZ coordinates

Table S5. XYZ coordinates of optimized structures.

Ligand	O	6.607996000000	-0.870802000000	2.799141000000
	O	-1.868118000000	-1.668900000000	-2.673142000000
	N	3.670860000000	-1.418487000000	1.357493000000
	N	1.043760000000	-1.099869000000	-1.126410000000
	N	5.246615000000	-2.453243000000	3.755481000000
	N	-0.481493000000	-0.064568000000	-3.551328000000
	C	5.473372000000	-1.350065000000	2.989607000000
	C	4.284849000000	-0.699952000000	2.310630000000
	C	3.936341000000	0.627378000000	2.623014000000
	H	4.478386000000	1.175688000000	3.406801000000
	C	2.879837000000	1.212140000000	1.911166000000
	H	2.561443000000	2.242281000000	2.131783000000
	C	2.235681000000	0.471180000000	0.912511000000
	H	1.406288000000	0.891504000000	0.328696000000
	C	2.668001000000	-0.847718000000	0.656512000000
	C	2.025309000000	-1.679739000000	-0.402530000000
	C	2.436851000000	-3.010401000000	-0.630406000000
	H	3.247934000000	-3.436888000000	-0.025126000000

	C	1.794126000000	-3.755274000000	-1.627298000000
	H	2.095762000000	-4.794743000000	-1.826652000000
	C	0.759947000000	-3.161697000000	-2.363335000000
	H	0.219198000000	-3.711096000000	-3.147312000000
	C	0.432358000000	-1.821860000000	-2.078423000000
	C	-0.731691000000	-1.172723000000	-2.798129000000
	C	3.903542000000	-2.951459000000	4.115075000000
	H	3.233421000000	-2.805843000000	3.248223000000
	H	3.999168000000	-4.045329000000	4.263617000000
	C	3.329736000000	-2.289068000000	5.366473000000
	H	3.220882000000	-1.195375000000	5.220437000000
	H	2.327945000000	-2.709632000000	5.586692000000
	H	3.975487000000	-2.461006000000	6.250434000000
	C	6.377650000000	-3.121901000000	4.345375000000
	C	6.945955000000	-4.225364000000	3.664186000000
	C	8.030370000000	-4.883065000000	4.280237000000
	C	7.961881000000	-3.357583000000	6.175962000000
	H	8.355560000000	-3.016983000000	7.145770000000
	C	6.880779000000	-2.686882000000	5.582574000000
	H	6.421624000000	-1.814979000000	6.071108000000
	C	6.411321000000	-4.665574000000	2.326497000000
	H	6.457971000000	-3.842219000000	1.583962000000
	H	6.988621000000	-5.522382000000	1.931985000000
	H	5.345694000000	-4.968781000000	2.392175000000
	C	0.860889000000	0.478270000000	-3.827690000000
	H	1.602559000000	-0.308556000000	-3.595361000000
	H	0.921546000000	0.658395000000	-4.921221000000
	C	1.177575000000	1.762236000000	-3.065350000000
	H	0.469465000000	2.574331000000	-3.324319000000
	H	1.136042000000	1.588591000000	-1.972719000000
	H	2.198250000000	2.106278000000	-3.327347000000
	C	-1.596506000000	0.594491000000	-4.182444000000
	C	-1.983364000000	0.207101000000	-5.488389000000
	C	-3.060578000000	0.898752000000	-6.079726000000
	H	-3.380177000000	0.613337000000	-7.094568000000
	C	-3.732062000000	1.929959000000	-5.402022000000
	H	-4.569790000000	2.450609000000	-5.891206000000
	C	-3.339831000000	2.290146000000	-4.102457000000
	H	-3.864878000000	3.092418000000	-3.561979000000
	C	-2.269375000000	1.616842000000	-3.493158000000
	H	-1.946728000000	1.875077000000	-2.473674000000
	C	-1.279920000000	-0.914151000000	-6.207303000000
	H	-1.762756000000	-1.124701000000	-7.179742000000
	H	-0.214136000000	-0.672363000000	-6.401554000000
	H	-1.288227000000	-1.845582000000	-5.604778000000
	C	8.534776000000	-4.460462000000	5.521531000000
	H	9.382758000000	-4.994438000000	5.977570000000
	H	8.488548000000	-5.744333000000	3.768573000000
$LNp^{V}O_2NO_3$	Np	-1.052441000000	-0.825095000000	-0.022397000000
	O	-0.840989000000	0.978708000000	-0.126032000000
	O	-1.268222000000	-2.627182000000	0.072794000000
	O	-1.188446000000	-0.660842000000	2.467042000000
	O	-1.188619000000	-0.960620000000	-2.527424000000
	O	-3.435983000000	-0.518695000000	1.052279000000
	O	-3.426963000000	-0.598924000000	-1.110454000000

	O	-5.329924000000	-0.331758000000	-0.045295000000
	N	1.177378000000	-1.050158000000	1.339886000000
	N	1.177469000000	-1.097101000000	-1.318548000000
	N	-0.278733000000	0.381556000000	4.277663000000
	N	-0.331171000000	0.221601000000	-4.282142000000
	N	-4.101793000000	-0.479365000000	-0.033547000000
	C	-0.177296000000	-0.369715000000	3.156985000000
	C	1.142757000000	-0.902854000000	2.683785000000
	C	2.191411000000	-1.317175000000	3.519074000000
	H	2.119402000000	-1.212145000000	4.608219000000
	C	3.323406000000	-1.893434000000	2.926228000000
	H	4.153150000000	-2.257712000000	3.548917000000
	C	3.391142000000	-1.985903000000	1.533016000000
	H	4.281699000000	-2.412267000000	1.053806000000
	C	2.301095000000	-1.537540000000	0.758942000000
	C	2.317845000000	-1.522673000000	-0.719515000000
	C	3.455233000000	-1.875436000000	-1.472754000000
	H	4.365836000000	-2.237080000000	-0.978325000000
	C	3.418588000000	-1.754294000000	-2.865839000000
	H	4.290902000000	-2.037067000000	-3.472384000000
	C	2.259508000000	-1.256197000000	-3.476812000000
	H	2.205339000000	-1.136931000000	-4.565731000000
	C	1.161648000000	-0.939529000000	-2.663129000000
	C	-0.191841000000	-0.538571000000	-3.171444000000
	C	-1.619767000000	0.862374000000	4.674982000000
	H	-2.337601000000	0.043375000000	4.480403000000
	H	-1.591949000000	1.039507000000	5.766012000000
	C	-2.022530000000	2.136174000000	3.933604000000
	H	-2.062905000000	1.965239000000	2.840370000000
	H	-3.026318000000	2.460433000000	4.272341000000
	H	-1.309000000000	2.959084000000	4.137172000000
	C	0.858228000000	1.007532000000	4.897864000000
	C	1.202084000000	0.684903000000	6.233412000000
	C	2.319048000000	1.344173000000	6.787349000000
	C	2.705058000000	2.582820000000	4.728293000000
	H	3.282631000000	3.314978000000	4.144324000000
	C	1.595194000000	1.948244000000	4.154531000000
	H	1.288104000000	2.172502000000	3.122100000000
	C	0.434532000000	-0.340229000000	7.025043000000
	H	0.095601000000	-1.179241000000	6.384938000000
	H	1.054164000000	-0.746911000000	7.846169000000
	H	-0.475185000000	0.100525000000	7.485629000000
	C	-1.698371000000	0.554747000000	-4.736049000000
	H	-1.645205000000	0.735084000000	-5.825687000000
	H	-2.329677000000	-0.337990000000	-4.568669000000
	C	-2.268077000000	1.775678000000	-4.015687000000
	H	-2.336172000000	1.598438000000	-2.925016000000
	H	-1.640376000000	2.671877000000	-4.190453000000
	H	-3.285823000000	1.989723000000	-4.397613000000
	C	0.753412000000	0.995395000000	-4.824249000000
	C	1.193950000000	0.768764000000	-6.150936000000
	C	2.251664000000	1.573296000000	-6.623577000000
	H	2.622880000000	1.407922000000	-7.647233000000
	C	2.849422000000	2.556252000000	-5.818944000000
	H	3.676752000000	3.161448000000	-6.220055000000

	C	2.396939000000	2.761747000000	-4.504785000000
	H	2.858473000000	3.529961000000	-3.866475000000
	C	1.342335000000	1.982193000000	-4.011363000000
	H	0.962878000000	2.127668000000	-2.988815000000
	C	0.588692000000	-0.303800000000	-7.017089000000
	H	1.295127000000	-0.613469000000	-7.810078000000
	H	0.305892000000	-1.196243000000	-6.423726000000
	H	-0.334784000000	0.053956000000	-7.520374000000
	C	3.064507000000	2.279579000000	6.052162000000
	H	3.934000000000	2.770508000000	6.515453000000
	H	2.616440000000	1.100442000000	7.819434000000
$[LNp^{VI}O_2NO_3]NO_3$	Np	-0.901122000000	-0.376911000000	0.040683000000
	O	-0.680548000000	1.384406000000	0.097546000000
	O	-1.101641000000	-2.138703000000	-0.016983000000
	O	-1.018717000000	-0.423198000000	2.406898000000
	O	-1.019848000000	-0.270726000000	-2.327328000000
	O	-3.219228000000	-0.159303000000	1.121387000000
	O	-3.212956000000	-0.070967000000	-1.029977000000
	O	-5.116951000000	0.112365000000	0.049478000000
	N	1.334963000000	-0.639920000000	1.371500000000
	N	1.329629000000	-0.642293000000	-1.307251000000
	N	-0.322759000000	0.353321000000	4.416570000000
	N	-0.279152000000	0.392405000000	-4.361681000000
	N	-3.899662000000	-0.033777000000	0.047184000000
	C	-0.069411000000	-0.180101000000	3.209806000000
	C	1.300111000000	-0.534119000000	2.721852000000
	C	2.411740000000	-0.820537000000	3.528036000000
	H	2.345708000000	-0.769777000000	4.620448000000
	C	3.610954000000	-1.185264000000	2.904660000000
	H	4.499975000000	-1.422143000000	3.505909000000
	C	3.664403000000	-1.239345000000	1.512002000000
	H	4.603670000000	-1.496449000000	1.009632000000
	C	2.495191000000	-0.976993000000	0.768557000000
	C	2.474667000000	-1.037170000000	-0.707854000000
	C	3.586251000000	-1.472239000000	-1.459033000000
	H	4.498288000000	-1.822406000000	-0.960688000000
	C	3.506634000000	-1.478688000000	-2.852074000000
	H	4.350613000000	-1.839871000000	-3.456815000000
	C	2.342217000000	-1.009600000000	-3.471789000000
	H	2.260926000000	-0.989467000000	-4.564413000000
	C	1.277703000000	-0.590273000000	-2.660040000000
	C	-0.062089000000	-0.131103000000	-3.143033000000
	C	-1.730971000000	0.654398000000	4.767549000000
	H	-2.355103000000	-0.176281000000	4.387809000000
	H	-1.788636000000	0.653347000000	5.871463000000
	C	-2.191804000000	1.997198000000	4.203861000000
	H	-2.137893000000	2.005362000000	3.098222000000
	H	-3.243519000000	2.176570000000	4.501770000000
	H	-1.575244000000	2.828864000000	4.597883000000
	C	0.695124000000	0.891738000000	5.281204000000
	C	0.967067000000	0.258574000000	6.518125000000
	C	1.963356000000	0.841196000000	7.327991000000
	C	2.365363000000	2.604731000000	5.697449000000
	H	2.903989000000	3.509453000000	5.378421000000
	C	1.376875000000	2.051289000000	4.872093000000

	H	1.127365000000	2.506973000000	3.902486000000
	C	0.256749000000	-1.002034000000	6.933335000000
	H	0.158346000000	-1.709629000000	6.085253000000
	H	0.800288000000	-1.506297000000	7.753779000000
	H	-0.771368000000	-0.790381000000	7.295555000000
	C	-1.659898000000	0.802466000000	-4.710782000000
	H	-1.725945000000	0.784838000000	-5.813998000000
	H	-2.347759000000	0.033700000000	-4.311229000000
	C	-2.004081000000	2.189450000000	-4.171383000000
	H	-1.943748000000	2.214393000000	-3.066283000000
	H	-1.321892000000	2.958782000000	-4.583562000000
	H	-3.038474000000	2.451004000000	-4.469107000000
	C	0.775526000000	0.826207000000	-5.240633000000
	C	0.978820000000	0.157625000000	-6.472222000000
	C	2.017796000000	0.638022000000	-7.295668000000
	H	2.210469000000	0.128517000000	-8.252683000000
	C	2.816268000000	1.728799000000	-6.915549000000
	H	3.622198000000	2.072795000000	-7.581581000000
	C	2.592369000000	2.374939000000	-5.688619000000
	H	3.213655000000	3.230283000000	-5.383984000000
	C	1.564019000000	1.923267000000	-4.850299000000
	H	1.364752000000	2.411182000000	-3.884781000000
	C	0.151842000000	-1.035267000000	-6.871426000000
	H	0.655561000000	-1.612459000000	-7.668924000000
	H	-0.034907000000	-1.707420000000	-6.009819000000
	H	-0.842172000000	-0.728656000000	-7.260544000000
	C	2.655945000000	1.996010000000	6.929465000000
	H	3.431611000000	2.420025000000	7.585221000000
	H	2.208303000000	0.362531000000	8.288923000000
	N	2.793409000000	-4.341994000000	1.622991000000
	O	2.721184000000	-4.566136000000	2.864046000000
	O	1.753437000000	-4.040332000000	0.973261000000
	O	3.908862000000	-4.408773000000	1.032404000000
$[LNp^{VI}O_2NO_3][Np^{VI}O_2(NO_3)_3]$	Np	-2.565174000000	-6.237400000000	-9.129109000000
	O	-2.151564000000	-4.524605000000	-8.917184000000
	O	-2.966922000000	-7.947018000000	-9.349571000000
	O	-2.683152000000	-6.551977000000	-6.800682000000
	O	-2.648790000000	-5.968047000000	-11.476641000000
	O	-4.837869000000	-5.840705000000	-8.027954000000
	O	-4.807283000000	-5.548487000000	-10.161900000000
	O	-6.681953000000	-5.240954000000	-9.059429000000
	N	-0.358999000000	-6.701309000000	-7.807389000000
	N	-0.387715000000	-6.712388000000	-10.502560000000
	N	-2.092543000000	-6.150996000000	-4.661863000000
	N	-1.960797000000	-5.775391000000	-13.619998000000
	N	-5.491767000000	-5.531495000000	-9.082566000000
	C	-1.763596000000	-6.380374000000	-5.943509000000
	C	-0.363692000000	-6.523649000000	-6.462102000000
	C	0.817261000000	-6.572067000000	-5.704686000000
	H	0.802533000000	-6.429092000000	-4.620492000000
	C	2.027743000000	-6.829141000000	-6.359378000000
	H	2.965829000000	-6.871239000000	-5.788141000000
	C	2.025300000000	-7.047088000000	-7.735753000000
	H	2.962384000000	-7.255107000000	-8.267166000000
	C	0.802833000000	-6.975477000000	-8.433826000000

	C	0.728715000000	-7.170953000000	-9.896753000000
	C	1.760601000000	-7.799200000000	-10.622498000000
	H	2.642302000000	-8.202099000000	-10.108122000000
	C	1.625163000000	-7.941436000000	-12.003774000000
	H	2.394569000000	-8.464595000000	-12.588986000000
	C	0.501626000000	-7.400139000000	-12.640022000000
	H	0.387425000000	-7.481729000000	-13.726326000000
	C	-0.477112000000	-6.771845000000	-11.854125000000
	C	-1.745448000000	-6.145379000000	-12.345718000000
	C	-3.531168000000	-6.117086000000	-4.302812000000
	H	-4.038108000000	-6.909135000000	-4.885405000000
	H	-3.589504000000	-6.384849000000	-3.231063000000
	C	-4.165357000000	-4.751008000000	-4.554334000000
	H	-4.108404000000	-4.477354000000	-5.625132000000
	H	-5.233353000000	-4.787705000000	-4.262119000000
	H	-3.672029000000	-3.962235000000	-3.953355000000
	C	-1.169846000000	-5.746735000000	-3.633035000000
	C	-0.766074000000	-6.688538000000	-2.656256000000
	C	0.116265000000	-6.231684000000	-1.656414000000
	C	0.154332000000	-3.989848000000	-2.609282000000
	H	0.510054000000	-2.948910000000	-2.593573000000
	C	-0.725683000000	-4.413750000000	-3.615466000000
	H	-1.065258000000	-3.724433000000	-4.402178000000
	C	-1.214484000000	-8.122830000000	-2.720089000000
	H	-0.952873000000	-8.583029000000	-3.694578000000
	H	-0.742327000000	-8.718400000000	-1.917498000000
	H	-2.314574000000	-8.217624000000	-2.614042000000
	C	-3.273398000000	-5.177460000000	-13.962429000000
	H	-3.421680000000	-5.343328000000	-15.045311000000
	H	-4.051723000000	-5.743104000000	-13.416460000000
	C	-3.337411000000	-3.687557000000	-13.632183000000
	H	-3.196173000000	-3.511798000000	-12.548434000000
	H	-2.565917000000	-3.120669000000	-14.189522000000
	H	-4.330956000000	-3.292496000000	-13.921807000000
	C	-0.928021000000	-5.686610000000	-14.619286000000
	C	-0.936107000000	-6.587909000000	-15.711368000000
	C	0.090103000000	-6.441735000000	-16.666924000000
	H	0.119330000000	-7.137652000000	-17.519761000000
	C	1.076207000000	-5.449375000000	-16.544156000000
	H	1.865963000000	-5.368376000000	-17.306528000000
	C	1.059581000000	-4.567194000000	-15.451299000000
	H	1.828994000000	-3.787506000000	-15.348681000000
	C	0.049227000000	-4.684700000000	-14.486808000000
	H	0.010529000000	-4.008996000000	-13.619661000000
	C	-1.965828000000	-7.679724000000	-15.825170000000
	H	-1.663372000000	-8.427373000000	-16.581500000000
	H	-2.116204000000	-8.196569000000	-14.855562000000
	H	-2.955309000000	-7.277497000000	-16.128589000000
	C	0.573368000000	-4.903742000000	-1.628574000000
	H	1.265504000000	-4.582453000000	-0.835366000000
	H	0.459108000000	-6.943572000000	-0.889568000000
	Np	-0.425146000000	-11.179775000000	-6.694895000000
	O	0.239247000000	-9.544684000000	-6.476954000000
	O	-1.085712000000	-12.821758000000	-6.907969000000
	O	-1.976254000000	-10.764270000000	-4.819108000000

	O	-2.688662000000	-10.195814000000	-6.781915000000
	O	-3.930412000000	-9.778513000000	-5.017661000000
	O	0.554352000000	-11.813566000000	-4.515767000000
	O	1.819317000000	-12.113796000000	-6.247107000000
	O	2.586996000000	-12.604511000000	-4.247095000000
	O	0.924626000000	-11.390595000000	-8.759134000000
	O	-1.083677000000	-10.621945000000	-9.007145000000
	O	0.214171000000	-10.842313000000	-10.765685000000
	N	-2.913230000000	-10.227397000000	-5.517154000000
	N	1.694612000000	-12.196559000000	-4.969888000000
	N	0.026103000000	-10.947886000000	-9.566012000000
$[LNp^{V}O_2NO_3]_2 \cdot Np^{VI}O_2(NO_3)_2$	Np	0.896550000000	7.846908000000	13.107759000000
	Np	0.752324000000	10.096302000000	9.408751000000
	O	0.893940000000	8.738237000000	11.517420000000
	O	0.909503000000	6.944402000000	14.658475000000
	O	2.549002000000	10.374462000000	9.418213000000
	O	-1.381341000000	8.621873000000	13.454804000000
	O	3.246153000000	7.343094000000	12.766888000000
	O	0.558004000000	10.004571000000	14.490582000000
	O	2.598895000000	9.602213000000	13.912446000000
	O	2.124233000000	11.463681000000	14.978317000000
	O	1.232659000000	7.580324000000	9.047172000000
	O	0.791370000000	8.690381000000	7.241352000000
	O	1.191816000000	6.533861000000	7.115747000000
	N	-1.058152000000	6.313242000000	12.251701000000
	N	1.497481000000	5.608438000000	11.872447000000
	N	-3.481302000000	8.947307000000	12.641417000000
	N	4.910323000000	6.642534000000	11.382062000000
	N	1.771512000000	10.395106000000	14.480376000000
	N	1.073318000000	7.567831000000	7.779632000000
	C	-2.393334000000	8.176812000000	12.847168000000
	C	-2.330125000000	6.746172000000	12.402345000000
	C	-3.438448000000	5.895610000000	12.262982000000
	H	-4.456717000000	6.264164000000	12.430430000000
	C	-3.211982000000	4.558139000000	11.921210000000
	H	-4.054676000000	3.859360000000	11.820113000000
	C	-1.902973000000	4.124526000000	11.702041000000
	H	-1.714273000000	3.083613000000	11.412910000000
	C	-0.838999000000	5.032787000000	11.876091000000
	C	0.572912000000	4.646716000000	11.655197000000
	C	0.940750000000	3.352901000000	11.232603000000
	H	0.183386000000	2.576781000000	11.068190000000
	C	2.291818000000	3.057040000000	11.041300000000
	H	2.604015000000	2.046307000000	10.741980000000
	C	3.242571000000	4.066507000000	11.226132000000
	H	4.308721000000	3.863561000000	11.074036000000
	C	2.798236000000	5.337241000000	11.625089000000
	C	3.688214000000	6.503089000000	11.935723000000
	C	-3.484018000000	10.320594000000	13.190788000000
	H	-2.961292000000	10.287001000000	14.164708000000
	H	-4.539015000000	10.590819000000	13.378651000000
	C	-2.832040000000	11.327444000000	12.248429000000
	H	-1.776901000000	11.065277000000	12.048613000000
	H	-2.860311000000	12.332106000000	12.711459000000
	H	-3.370025000000	11.381734000000	11.282996000000

	C	-4.486832000000	8.610008000000	11.668995000000
	C	-5.830299000000	8.416799000000	12.075058000000
	C	-6.755880000000	8.059453000000	11.073160000000
	H	-7.804381000000	7.886976000000	11.362564000000
	C	-6.366995000000	7.887147000000	9.734921000000
	H	-7.114929000000	7.592040000000	8.983187000000
	C	-5.028551000000	8.085386000000	9.359542000000
	H	-4.715351000000	7.955911000000	8.313250000000
	C	-4.088548000000	8.462429000000	10.327542000000
	H	-3.038864000000	8.651912000000	10.053981000000
	C	-6.255300000000	8.531643000000	13.515058000000
	H	-5.467605000000	8.165352000000	14.203463000000
	H	-7.180789000000	7.953600000000	13.696582000000
	H	-6.465898000000	9.585453000000	13.795341000000
	C	5.746014000000	7.788798000000	11.800830000000
	H	6.800416000000	7.466758000000	11.721019000000
	H	5.528031000000	7.982371000000	12.867224000000
	C	5.498419000000	9.030098000000	10.950353000000
	H	4.445048000000	9.363145000000	11.008050000000
	H	5.744100000000	8.845817000000	9.886302000000
	H	6.145375000000	9.853288000000	11.308287000000
	C	5.305135000000	5.934986000000	10.192986000000
	C	6.435227000000	5.081495000000	10.217377000000
	C	6.760187000000	4.414782000000	9.017923000000
	H	7.625276000000	3.733303000000	9.012133000000
	C	5.994749000000	4.575921000000	7.852011000000
	H	6.271103000000	4.028843000000	6.937727000000
	C	4.876319000000	5.425066000000	7.855586000000
	H	4.268543000000	5.555571000000	6.948465000000
	C	4.538897000000	6.115360000000	9.026615000000
	H	3.670780000000	6.790380000000	9.052742000000
	C	7.234803000000	4.847884000000	11.471823000000
	H	7.747321000000	3.868332000000	11.431143000000
	H	6.594520000000	4.875993000000	12.375814000000
	H	8.019246000000	5.622917000000	11.604569000000
	Np	0.605996000000	12.322489000000	5.696387000000
	O	0.617062000000	11.454590000000	7.303582000000
	O	0.593348000000	13.208990000000	4.132928000000
	O	-1.044238000000	9.817026000000	9.401841000000
	O	2.892814000000	11.555444000000	5.347916000000
	O	-1.751528000000	12.828632000000	6.017036000000
	O	0.955014000000	10.156726000000	4.317163000000
	O	-1.084680000000	10.543584000000	4.913426000000
	O	-0.603462000000	8.683353000000	3.848805000000
	O	0.270247000000	12.610621000000	9.766863000000
	O	0.707190000000	11.505854000000	11.576985000000
	O	0.302944000000	13.662034000000	11.695590000000
	N	2.555925000000	13.864280000000	6.552651000000
	N	-0.003354000000	14.564824000000	6.921010000000
	N	4.986992000000	11.235856000000	6.179112000000
	N	-3.413647000000	13.524690000000	7.406899000000
	N	-0.254816000000	9.756810000000	4.340348000000
	N	0.425322000000	12.626559000000	11.034730000000
	C	3.898397000000	12.003261000000	5.963425000000
	C	3.829337000000	13.434513000000	6.406687000000

	C	4.935308000000	14.287689000000	6.548689000000
	H	5.954959000000	13.921437000000	6.384520000000
	C	4.704605000000	15.624916000000	6.888858000000
	H	5.545276000000	16.325818000000	6.992141000000
	C	3.393853000000	16.055493000000	7.103477000000
	H	3.202035000000	17.096269000000	7.391063000000
	C	2.332553000000	15.144580000000	6.926473000000
	C	0.918875000000	15.528201000000	7.141298000000
	C	0.547006000000	16.821899000000	7.560841000000
	H	1.302167000000	17.599521000000	7.728308000000
	C	-0.805397000000	17.116133000000	7.745237000000
	H	-1.120386000000	18.126784000000	8.041914000000
	C	-1.753860000000	16.105098000000	7.556751000000
	H	-2.821053000000	16.306735000000	7.703234000000
	C	-1.305463000000	14.834557000000	7.161836000000
	C	-2.193226000000	13.666865000000	6.849863000000
	C	4.996449000000	9.861761000000	5.632145000000
	H	4.485477000000	9.893476000000	4.651919000000
	H	6.053609000000	9.591155000000	5.457410000000
	C	4.333425000000	8.856357000000	6.568237000000
	H	3.276411000000	9.119516000000	6.756354000000
	H	4.366227000000	7.851013000000	6.106993000000
	H	4.860877000000	8.803054000000	7.539482000000
	C	5.985464000000	11.577454000000	7.157275000000
	C	7.331122000000	11.772275000000	6.759216000000
	C	8.250113000000	12.132727000000	7.766057000000
	H	9.300152000000	12.306042000000	7.482752000000
	C	7.853011000000	12.306012000000	9.101734000000
	H	8.596043000000	12.602942000000	9.857608000000
	C	6.512692000000	12.105702000000	9.469295000000
	H	6.192846000000	12.235419000000	10.513601000000
	C	5.579124000000	11.726135000000	8.496084000000
	H	4.528532000000	11.534201000000	8.764098000000
	C	7.765081000000	11.654671000000	5.322103000000
	H	6.981528000000	12.019518000000	4.628204000000
	H	8.691640000000	12.232383000000	5.145065000000
	H	7.977242000000	10.600327000000	5.045019000000
	C	-4.246965000000	12.375691000000	6.991104000000
	H	-5.302287000000	12.693280000000	7.076262000000
	H	-4.033258000000	12.183506000000	5.923577000000
	C	-3.989716000000	11.135124000000	7.839879000000
	H	-2.935148000000	10.806991000000	7.776569000000
	H	-4.230566000000	11.318240000000	8.905218000000
	H	-4.634707000000	10.309120000000	7.484953000000
	C	-3.807705000000	14.231305000000	8.596804000000
	C	-4.940039000000	15.081945000000	8.574322000000
	C	-5.264841000000	15.747918000000	9.774208000000
	H	-6.131679000000	16.427150000000	9.781350000000
	C	-4.497238000000	15.588619000000	10.938978000000
	H	-4.773518000000	16.134944000000	11.853730000000
	C	-3.376886000000	14.742042000000	10.933688000000
	H	-2.767417000000	14.613055000000	11.839843000000
	C	-3.039489000000	14.052598000000	9.762123000000
	H	-2.169762000000	13.379615000000	9.734860000000
	C	-5.742482000000	15.313070000000	7.321206000000

	H	-6.259285000000	16.290292000000	7.363417000000
	H	-5.103322000000	15.288408000000	6.416288000000
	H	-6.523641000000	14.534682000000	7.188687000000

References

1 N. E. Borisova, A. M. Fedoseev, G. V. Kostikova, P. I. Matveev, L. Y. Starostin, M. N. Sokolova and M. V. Evsiunina, Solvent Extraction and Conformation Rigidity: Actinide(IV) and Actinide(VI) Come Together, *Inorg. Chem.*, 2022, **61**, 20774–20784.

2 M. Y. Alyapyshev, V. A. Babain, L. I. Tkachenko, A. Paulenova, A. A. Popova and N. E. Borisova, New Diamides of 2,2′-dipyridyl-6,6′-dicarboxylic Acid for Actinide-Lanthanide Separation, *Solvent Extraction and Ion Exchange*, 2014, **32**, 138–152.

3 L. Krause, R. Herbst-Irmer, G. M. Sheldrick and D. Stalke, Comparison of silver and molybdenum microfocus X-ray sources for single-crystal structure determination, *J. Appl. Crystallogr.*, 2015, **48**, 3–10.

4 G. M. Sheldrick, SHELXT - Integrated space-group and crystal-structure determination, *Acta Crystallogr. A*, 2015, **71**, 3–8.

5 G. M. Sheldrick, Crystal structure refinement with SHELXL, *Acta Crystallogr.*, 2015, C**71**, 3–8.

6 A. L. Spek, PLATON SQUEEZE: a tool for the calculation of the disordered solvent contribution to the calculated structure factors, *Acta Crystallogr.,* 2015, C**71** 9–18.

7 O. V. Dolomanov, L. J. Bourhis, R. J. Gildea, J. A. K. Howard and H. Puschmann, OLEX2: A complete structure solution, refinement and analysis program, *J. Appl. Crystallogr.*, 2009, **42**, 339–341.

8 A. A. Chernyshov, A. A. Veligzhanin and Y. V. Zubavichus, Structural Materials Science end-station at the Kurchatov Synchrotron Radiation Source: Recent instrumentation upgrades and experimental results, *Nucl. Instrum. Methods Phys. Res. A*, 2009, **603**, 95–98.

9 B. Ravel and M. Newville, ATHENA, ARTEMIS, HEPHAESTUS: Data analysis for X-ray absorption spectroscopy using IFEFFIT, *J. Synchrotron Radiat.*, 2005, **12**, 537–541.

10 A. L. Smith, P. Martin, D. Prieur, A. C. Scheinost, P. E. Raison, A. K. Cheetham and R. J. M. Konings, Structural Properties and Charge Distribution of the Sodium Uranium, Neptunium, and Plutonium Ternary Oxides: A Combined X-ray Diffraction and XANES Study, *Inorg. Chem.*, 2016, **55**, 1569–1579.

11 A. Ankudinov and B. Ravel, Real-space multiple-scattering calculation and interpretation of x-ray-absorption near-edge structure, *Phys. Rev. B Condens. Matter. Phys*, 1998, **58**, 7565–7576.

12 D. Novichkov, A. Trigub, E. Gerber, I. Nevolin, A. Romanchuk, P. Matveev and S. Kalmykov, Laboratory-based X-ray spectrometer for actinide science, *J. Synchrotron Radiat.*, 2023, **30**, 1114–1126.

13 S. Grimme, J. Antony, S. Ehrlich and H. Krieg, A consistent and accurate ab initio parametrization of density functional dispersion correction (DFT-D) for the 94 elements H-Pu, *Journal of Chemical Physics*, 2010, **132**, 154104.

14 S. Grimme, S. Enrlich and L. Goerigk, Effect of the Damping Function in Dispersion Corrected Density Functional Theory, *J. Comput. Chem.*, 2010, **32**, 1456–1465.

15 X. Cao, M. Dolg and H. Stoll, Valence basis sets for relativistic energy-consistent small-core actinide pseudopotentials, *Journal of Chemical Physics*, 2003, **118**, 487–496.

16 W. Küchle, M. Dolg, H. Stoll and H. Preuss, Energy-adjusted pseudopotentials for the actinides. Parameter sets and test calculations for thorium and thorium monoxide, *J. Chem. Phys.*, 1994, **100**, 7535–7542.

17 X. Cao and M. Dolg, Segmented contraction scheme for small-core actinide pseudopotential basis sets, *Journal of Molecular Structure: THEOCHEM*, 2004, **673**, 203–209.

18 Y. J. Franzke, R. Treß, T. M. Pazdera and F. Weigend, Error-consistent segmented contracted all-electron relativistic basis sets of double- and triple-zeta quality for NMR shielding constants, *Physical Chemistry Chemical Physics*, 2019, **21**, 16658–16664.

19 P. Pollak and F. Weigend, Segmented Contracted Error-Consistent Basis Sets of Double- and Triple-ζ Valence Quality for One- and Two-Component Relativistic All-Electron Calculations, *J. Chem. Theory Comput.*, 2017, **13**, 3696–3705.

20 S. V. Gutorova, P. I. Matveev, P. S. Lemport, A. L. Trigub, A. S. Pozdeev, A. V. Yatsenko, B. N. Tarasevich, E. A. Konopkina, E. K. Khult, V. A. Roznyatovsky, Y. V. Nelyubina, K. L. Isakovskaya, V. N. Khrustalev, V. S. Petrov, A. S. Aldoshin, Y. A. Ustynyuk, V. G. Petrov, S. N. Kalmykov and V. G. Nenajdenko, Structural Insight into Complexation Ability and Coordination of Uranyl Nitrate by 1,10-Phenanthroline-2,9-diamides, *Inorg. Chem.*, 2022, **61**, 384–398.

21 P. S. Lemport, M. V. Evsiunina, P. I. Matveev, V. S. Petrov, A. S. Pozdeev, E. K. Khult, Y. V. Nelyubina, K. L. Isakovskaya, V. A. Roznyatovsky, I. P. Gloriozov, B. N. Tarasevich, A. S. Aldoshin, V. G. Petrov,

S. N. Kalmykov, Y. A. Ustynyuk and V. G. Nenajdenko, 2-Methylpyrrolidine derived 1,10-phenanthroline-2,9-diamides: promising extractants for Am(III)/Ln(III) separation, *Inorg. Chem. Front.*, 2022, **9**, 4402–4412.

22 A. S. Pozdeev and I. A. Popov, The structural and electronic split: Boron vs aluminum hydrides, *Chemical Physics Reviews*, 2024, **5**, 011401.

23 Y. A. Ustynyuk, P. S. Lemport, V. A. Roznyatovsky, K. A. Lyssenko, A. O. Gudovannyy, P. I. Matveev, E. K. Khult, M. V. Evsiunina, V. G. Petrov, I. P. Gloriozov, A. S. Pozdeev, V. S. Petrov, N. A. Avagyan, A. S. Aldoshin, S. N. Kalmykov and V. G. Nenajdenko, First Trifluoromethylated Phenanthrolinediamides: Synthesis, Structure, Stereodynamics and Complexation with Ln(III), *Molecules*, 2022, **27**, 1–18.

24 O. Bunau, A. Y. Ramos and J. Y., The FDMNES code, *International Tables For Crystallography*, 2024, **1**, 752–757.